

Simulations of a multi-layer extended gating grid

J.D. Mulligan

Yale University, New Haven, CT, USA

Abstract

A novel idea to control ion back-flow in time projection chambers is to use a multi-layer extended gating grid to capture back-flowing ions at the expense of live time and electron transparency. In this initial study, I perform simulations of a four-layer grid for the ALICE and STAR time projection chambers, using Ne – CO₂ (90 – 10) and Ar – CH₄ (90 – 10) gas mixtures, respectively. I report the live time and electron transparency for both 90% and 99% ion back-flow suppression. Additionally, for the ALICE configuration I study several effects: using a mesh vs. wire-plane grid, including a magnetic field, and varying the over-voltage distribution in the gating region. For 90% ion back-flow suppression, I achieve 75% live time with 86% electron transparency for ALICE, and 95% live time with 83% electron transparency for STAR.

Keywords: Gating grid, Time projection chamber, Ion back-flow

1. Introduction

In high-rate gaseous time projection chambers (TPCs), ion back-flow (IBF) from the gas amplification region to the drift volume distorts the drift field, deteriorating tracking and PID performance. A recent proposal to control IBF in TPCs is to use a multi-layer extended gating grid [1]. In comparison to a traditional gating grid, the extension of the grid with multiple layers allows a longer time for ions to drift through the gate, while still collecting the ions quickly. The operating principle is that the gate remains transparent to electrons until the ion drift time exceeds the grid length (divided by the ion drift velocity), at which point the gate is closed and the ions are collected. Enhanced IBF suppression comes at the sacrifice of live time and electron transparency; for a given IBF tolerance, the design goal is to increase the live time fraction A while maintaining sufficient electron transparency for reconstruction performance. Such a design could operate as a primary means of IBF suppression, or in cooperation with other elements such as Gas Electron Multipliers. Early work suggests that for a wire-plane gate, low-field regions between the wires prevent some ions from being captured quickly [1]. The detailed simulations presented below quantify this effect and serve as an initial study of the general feasibility of a multi-layer extended gating grid.

Email address: james.mulligan@yale.edu (J.D. Mulligan)

2. Simulation Configurations

In order to study the performance of the grid in various TPC conditions, I simulate the gating region for two large gas TPCs: ALICE [2] and STAR [3]. These TPCs use different gas mixtures (with significantly different ion mobilities) and different drift fields, which considerably impact the gating performance.

In both TPC configurations, I consider a four-layer grid (Fig. 1), with the open field E_o parallel/anti-parallel to the closed field E_c . The spacing between layers is 3 mm, and the inter-layer wire spacing is 2 mm. I use a 3 mm drift volume above the grid, and a grounded plane 3 mm below the grid. The wire diameter is 100 μm . The ions are collected on the first and third planes from the gas amplification region, with $E_c \approx 2 \text{ kV/cm}$.

The fields are constructed using the finite element method software ANSYS [4]; the electron and ion drifts are simulated using Garfield++ [5]. Collision-level tracking is performed for electrons (“microscopic tracking”), and a more coarse-grained Monte Carlo tracking is used for ions. Diffusion is included for both electrons and ions. It should be noted that while Garfield++ can natively solve 2D fields, close examination revealed that the ANSYS solution is more accurate near the wires.

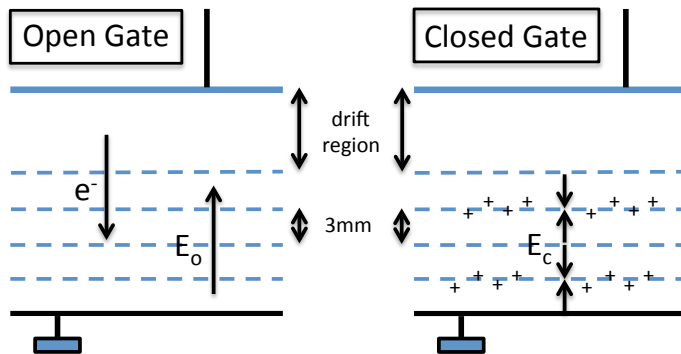


Figure 1: Schematics of the open (left) and closed (right) gating configurations. In the open configuration, electrons pass through with small losses, while positive ions back-drift through the gate. In the closed configuration, these back-drifted positive ions are collected on the first and third planes by E_c .

2.1. ALICE TPC

For the ALICE TPC, I use a gas mixture of Ne–CO₂ (90–10), as configured for LHC Run 1. The drift field is $\approx 0.4 \text{ kV/cm}$; a representative voltage switch required on the four gating planes (in volts) is: $(-600, 0, -600, 0) \leftrightarrow (-120, -240, -360, -480)$. The electron drift velocity in this mixture for the considered drift field is $2.73 \text{ cm}/\mu\text{s}$ [6]. Binary ion mobilities from the literature are linearly extrapolated to low fields and combined for the gas mixture using Blanc’s Law [7][8][9]. The dominant ion in this mixture is CO₂⁺ [10].

To study differences in ion collection time and electron transparency, I study separately a wire configuration and a mesh configuration (Fig. 2). The final finite element meshes contain approximately $3 \cdot 10^5$ elements for the wire configuration unit cell, and $2 \cdot 10^6$ elements for the mesh configuration unit cell. These correspond to an average element size of 56 μm for the wire configuration, and 33 μm for the mesh configuration.

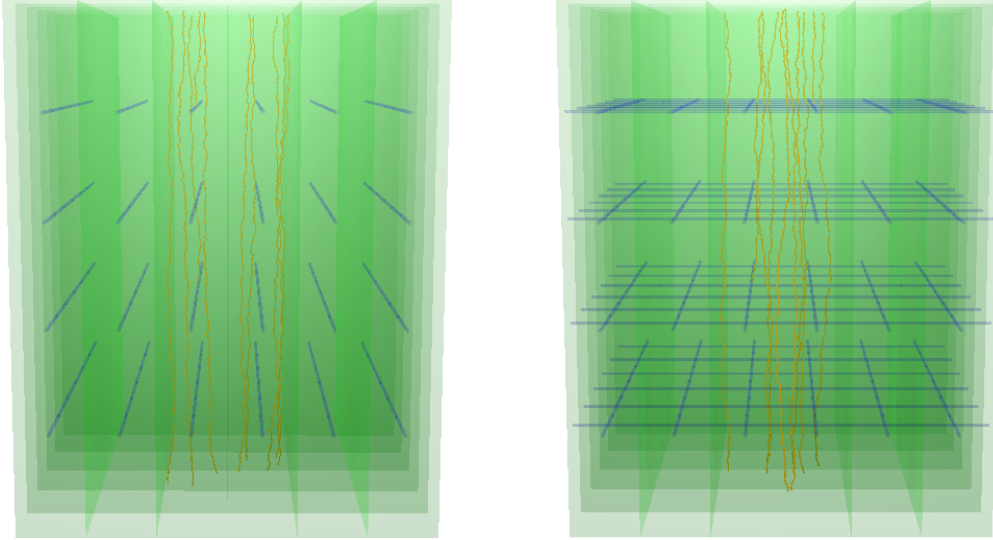


Figure 2: Visualizations of the multi-layer extended gating grids in the open configuration, with electron drift lines traveling downward. Plotted are 6×6 arrays of $2\text{mm} \times 2\text{mm} \times 15\text{mm}$ unit cells used for the simulation. Left: Wire-plane configuration. Right: Mesh configuration. Mesh spacing in-plane is 2 mm.

However, adaptive meshing is employed, which creates finer elements near geometrical features. The final meshes were examined for quality, and an informal convergence study was performed, in which iteratively refined meshes were produced, and the maximum field near the wires showed convergence to $< 10\%$.

2.2. STAR TPC

For the STAR TPC, I use a gas mixture of Ar – CH₄ (90 – 10). The drift field is approximately 140 V/cm. The electron drift velocity in this mixture for the considered drift field is 5.45 cm/ μs , and the ion mobility 1.6 cm²/V · s.

Only a wire-plane configuration is simulated. The finite element mesh contains approximately $3 \cdot 10^5$ elements for the unit cell, as for the ALICE wire-plane mesh.

3. Simulation Results – ALICE TPC

3.1. Electron Transparency

I measure electron transparency by randomly placing electrons at the top of the drift region, and measuring the fraction that pass through the grid in the open configuration. At each layer in the grid, I increment the field by a value ΔE in order to boost the transparency; increasing ΔE amounts to putting negative charge on the wires, which repels drifting electrons. I use fixed over-voltages corresponding to $\Delta E = 0, 10, 20, 30$ V/cm across each plane, yielding average open gating fields of $E_o = 400, 425, 450, 475$ V/cm. Figure 3 shows the results for both the wire-plane and mesh configurations.

Additionally, I repeated electron transparency measurement in the mesh configuration with a magnetic field $B = 0.5$ T parallel to the electric field. This results in a slight

Electron transparency vs. ΔE

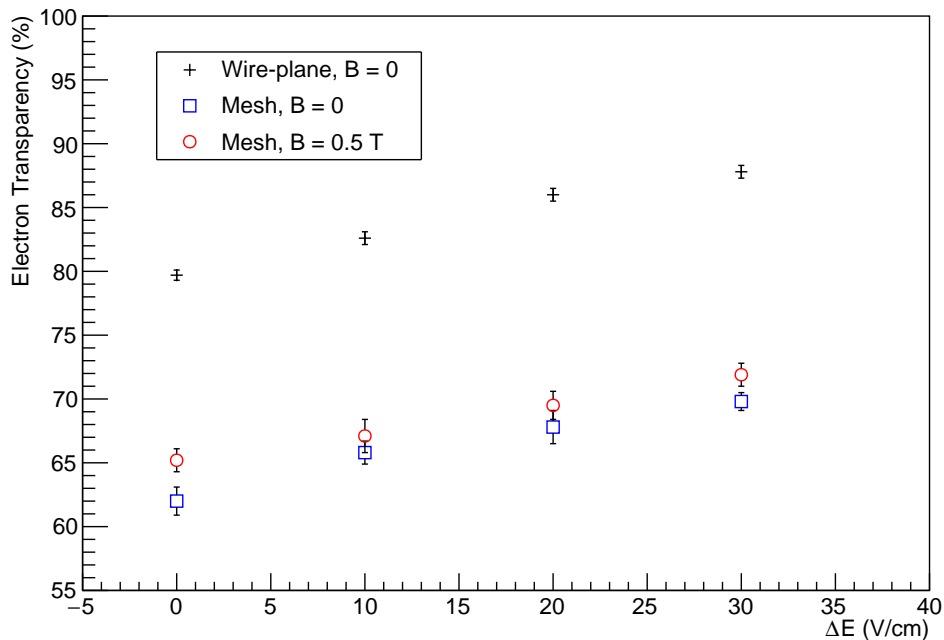


Figure 3: Electron transparency as a function of field incrementation ΔE at each layer of the grid, in the ALICE configuration. The error bars estimate the statistical uncertainty. For the wire-plane configuration, each point corresponds to $2.5 \cdot 10^4$ electrons. For the mesh configuration, each point corresponds to 10^4 electrons.

increase in transparency (Fig. 3), which may be due to reduced transverse diffusion (from the B -field) outweighing $E \times B$ effects (which may deviate drifting electrons from the electric field lines into a wire); the cause remains to be investigated.

Next, I examined the over-voltage distribution to determine if there is an optimal way to distribute ΔE over different planes, rather than fixing it to be constant across each layer. A comparison of fixed ΔE over each plane against having nonzero ΔE only across the first plane shows little difference (Fig. 4). In the latter case, fewer electrons are captured on the first layer, but more are captured in subsequent layers. This suggests that if more layers are added to the grid, the fixed ΔE configuration is better.

3.2. Live Time and Ion Collection

Following [1], the live time fraction A of the gating grid can be written

$$A = \frac{T_{active}}{T_{cycle}} = \frac{T_o - T_e}{T_o + T_c},$$

where T_o is the open time, T_c is the closed time, and T_e is the time for an electron to drift the length of the chamber. For a gating grid of N planes, layer separation Δh ,

Electron transparency vs. ΔE , Mesh Config

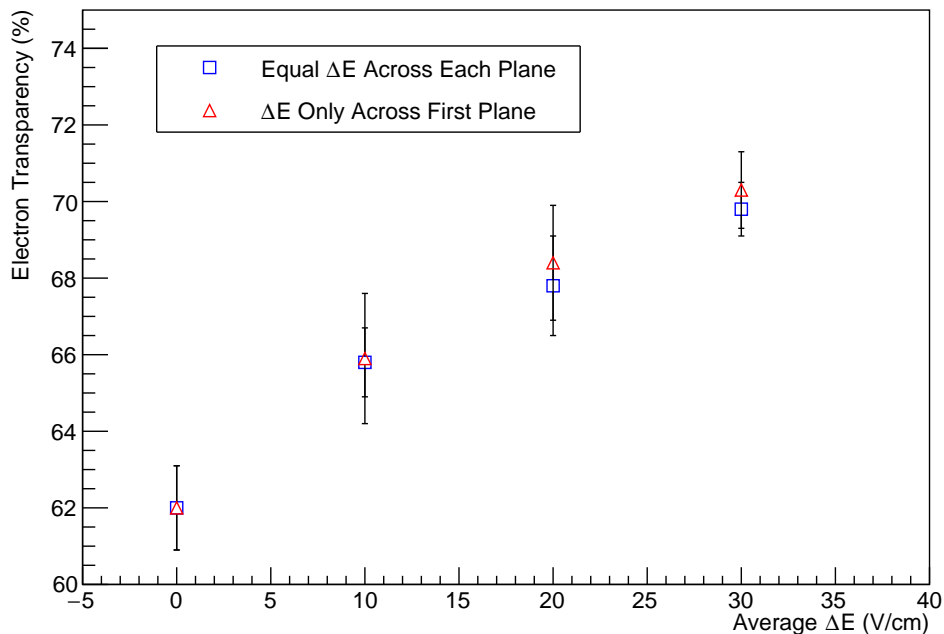


Figure 4: Electron transparency as a function of average ΔE across each layer of the grid, for two different overvoltage distributions, in the ALICE configuration. Each point corresponds to 10^4 electrons; the error bars estimate the statistical uncertainty.

ion mobility K_I , closed field E_c , average drift field within grid E_o , drift length L_e , and electron drift velocity v_e , these times can be estimated as:

$$\begin{aligned}
 T_o &= \frac{N\Delta h}{K_I E_o}, \\
 T_c &= \alpha \frac{\Delta h}{K_I E_c}, \\
 T_e &= \frac{L_e}{v_e}.
 \end{aligned}$$

The factor α in the collection time accounts for the fact that the field is not from parallel plates, but rather has low-field regions in between the wires due to saddle points in the potential. Therefore α depends on the IBF threshold imposed. From the above expressions, the live time can be written:

$$A = \frac{1 - \frac{E_o K_I L_e}{N\Delta h v_e}}{1 + \alpha \frac{E_o}{N E_c}}. \quad (1)$$

This makes clear the dependence of the live time on various detector parameters. The

present simulations involve the following parameter values, determined with the ALICE TPC in mind:

Param	Estimated value	$A \uparrow$ if	Physical reason	Constrained by
N	4	\uparrow	Longer T_o	Transparency
Δh	3 mm	\uparrow	Longer T_o, T_c ; fixed T_e	Voltage; transparency
E_o	400 – 475 V/cm	\downarrow	Longer T_o	Transparency
E_c	2000 V/cm	\uparrow	Faster collection	Voltage
K_I	4.8 cm ² /V · s	\downarrow	Longer T_o, T_c ; fixed T_e	Gas choice
v_e	2.73 cm/ μ s	\uparrow	Smaller T_e	Gas choice
L_e	250 cm	\downarrow	Smaller T_e	Detector size
α	1 – 4	\downarrow	Longer collection time	IBF tolerance
w	2 mm	\downarrow	Smaller saddle area	Transparency

3.2.1. Ion Collection

To estimate the live time of the simulated configuration, the parameter α must be measured in simulation, or equivalently T_c . I measure the ion collection time by randomly (uniformly) placing ions in the gating region, as one would expect for backdrifting ions, and counting the time it takes to collect the ions in the closed configuration. Figure 5 shows the results.

Note that a constant plateau out to $t = \frac{\Delta h}{K_I E_c} \approx 31 \mu\text{s}$ exists for both cases (as expected from a parallel plate solution), while the wire configuration has a significantly longer tail, due to more low-field regions.

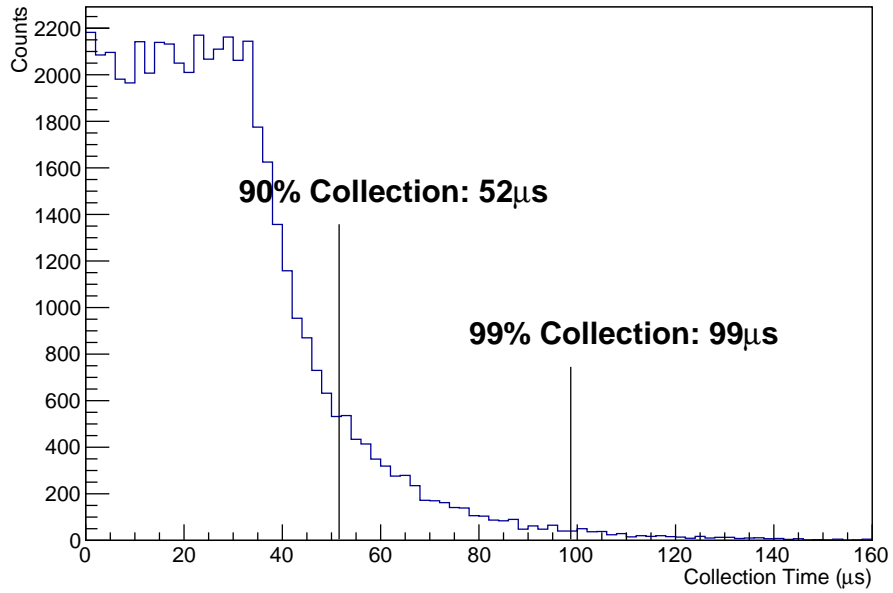
Additionally, I introduced a magnetic field $B = 0.5 \text{ T}$ in the mesh configuration, and repeated the ion collection. This causes no change in collection times, as expected since the magnetic force on ions is negligible due to their slow drift velocities (and additionally, the magnetic field would perturb ion trajectories not only into the low-field regions, but out of them as well).

3.2.2. Live Time Estimates

The measured collection times, in conjunction with the above table of parameters, yield the following live times, reported for 90% and 99% IBF, and for transparencies corresponding to $\Delta E = 0, 20 \text{ V/cm}$, for both the wire-plane and mesh configurations:

	Wire Configuration	Mesh Configuration
$E_o = 400 \text{ V/cm}$	(80% transparency)	(62% transparency)
99% IBF	73%	77%
90% IBF	78%	80%
$E_o = 450 \text{ V/cm}$	(86% transparency)	(68% transparency)
99% IBF	70%	74%
90% IBF	75%	78%

Ion Collection Time, Wire Config



Ion Collection Time, Mesh Config

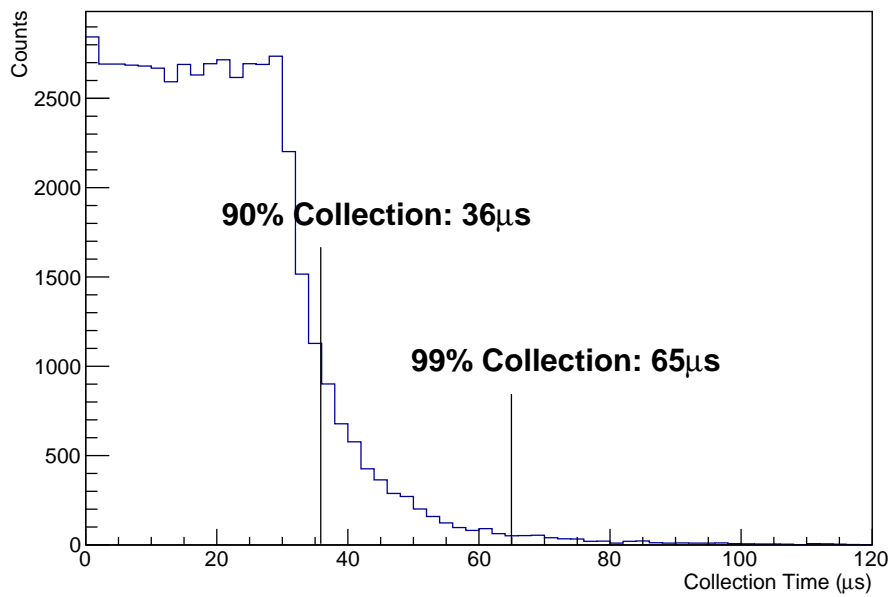


Figure 5: Histograms of $5 \cdot 10^4$ ion collection times in the ALICE configuration. The 90% and 99% IBF thresholds are illustrated. Top: Wire-plane configuration. Bottom: Mesh configuration.

4. Simulation Results – STAR TPC

Recalling equation (1), the corresponding table of values for STAR is estimated to be:

Param	Estimated value
N	4
Δh	3 mm
E_o	190 V/cm
E_c	2000 V/cm
K_I	1.6 cm ² /V · s
v_e	5.45 cm/ μ s
L_e	209 cm
α	2
w	2 mm

I take $E_o = 190$ V/cm, corresponding to a 140 V/cm drift field plus 20 V/cm per plane overvoltage. I then measure the electron transparency with this overvoltage via simulation of 25,000 electrons in the wire-plane configuration to be:

$$82.6\%.$$

The statistical error is $\approx \sqrt{np(1-p)}/n \approx 0.2\%$, but the dominant uncertainty is expected to come from the field map or one of many other possible sources of error, which haven't been quantified. The transparency could be boosted at the expense of live time by increasing the average gate field E_o . Also, small improvements $\sim 1\%$ were observed in ALICE simulations when a magnetic field was included, although this was not done here (the electrons in STAR are hotter than in ALICE, so the diffusion and $E \times B$ effects are both probably larger, and one would need to verify the outcome of their balance).

I measure the parameter α by simulating the ion collection time for 90% and 99% of backdrifting ions (Fig. 6). Recall that $\alpha = 2$ means that the closed time is equal to twice that of a perfect parallel plate. I find

$$\alpha_{90\%} = 1.6, \quad \alpha_{99\%} = 2.9.$$

The live time for this set of parameters, with 82.6% electron transparency, is then:

$$A_{90\%} = 95\%, \quad A_{99\%} = 93\%.$$

Relative to ALICE, the smaller drift field and the smaller ion mobility allow the open gate to be open longer (since ions drift back more slowly), and additionally the larger electron drift velocity reduces the electron drift time per cycle T_e . Note also that in this scheme, the detector could operate continuously for up to $T_o \sim 4$ ms before the gate needs to be closed.

5. Discussion

The results above provide an early quantitative look at possible modified gating grid configurations. The specific results for live time and electron transparency should not

Ion Collection Time, P10

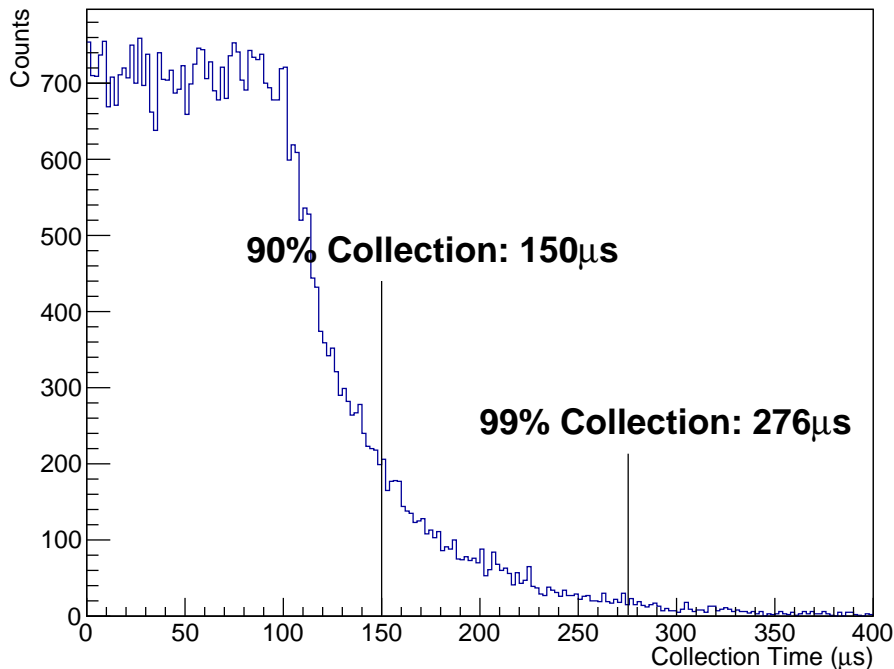


Figure 6: Histogram of $5 \cdot 10^4$ ion collection times in the STAR wire-plane configuration. The 90% and 99% IBF thresholds are illustrated.

be viewed as expected limits, but rather starting points from which optimization could begin.

One concrete conclusion, however, is that the mesh grid appears untenable. The idea of the mesh configuration is to increase the live time A by decreasing T_c , at the expense of transparency. However, the simulations suggest that the transparency cost is large for only a small improvement in live time. Further, it should be noted that the wire configuration has an additional advantage in that it preserves momentum information along the direction of the wires, whereas the mesh distorts momentum information in both directions. If one is determined to reduce T_c , an additional avenue to pursue is a dynamically switched gating cycle, in which the saddle point ions are swept out of the low-field region. This could be accomplished by the closed time consisting of two periods of $E_c \parallel E_o$ interspersed with a period of $E_c \perp E_o$.

A handful of additional parameters directly exhibit a tradeoff between live time and electron transparency: N , Δh , and E_o . The idea in designing a detector is to favor those variables that give maximal live time boost with minimal transparency loss.

If electron transparency is a concern, one should increase E_o as much as possible. To boost the live time, equation (1) suggests it is better to try to increase T_o rather than decrease T_c . Further study of varying N , Δh , and E_o should be undertaken. For example, in the ALICE configuration, plots of the final positions of electrons show that

transparency would decrease by approximately 3–5% if another layer is added to the grid. This extra layer will cause $T_o \rightarrow \frac{5}{4}T_o$, yielding live time improvements of approximately 5%. Adding yet another layer would have an even smaller effect on transparency, and yield a further boost in live time. Similar arguments can be made for increasing Δh , at the expense of longer collection time, perhaps worse transparency, and larger voltage switches. This option may be particularly attractive for situations in which 90% IBF suppression is acceptable. The possibility of significantly increasing E_o in concert with these approaches may be particularly appealing, and should be tested.

To estimate the live time for configurations other than ALICE or STAR, one can use equation (1), upon choosing an α comparable to those for the ALICE and STAR results (for a given IBF suppression). Electron transparency estimates are more difficult, and require detailed simulation.

6. Conclusions

The presented simulations suggest that a multi-layer extended gating grid may be a feasible option for reducing IBF in TPCs, depending on acceptable losses of live time and electron transparency, and the TPC configuration. There remains significant room for optimization, and it is expected that results will continue to improve as they are adapted for particular applications. Experimental tests are also being pursued.

7. Acknowledgements

Thanks to H. Wieman, J.W. Harris, R. Majka, and N. Smirnov for guidance and valuable discussions. Thanks also to the Garfield++ developers for providing helpful documentation and useful examples from which to learn.

This work was supported by the US Department of Energy under Grant DE-SC004168.

This work was supported in part by the facilities and staff of the Yale University Faculty of Arts and Sciences High Performance Computing Center.

References

- [1] H. Wieman, Gating grid concept for alice upgrade (2014).
URL https://wiki.bnl.gov/eic/upload/Alice_upgrade_gating_grid_idea.pdf
- [2] Alice.
URL <http://alice-collaboration.web.cern.ch>
- [3] Star.
URL <https://www.star.bnl.gov>
- [4] Ansys.
URL <http://www.ansys.com>
- [5] Garfield++.
URL <http://garfieldpp.web.cern.ch>
- [6] ALICE Collaboration, Technical design report for the upgrade of the alice time projection chamber ALICE-TDR-016 (2014) p. 14 Table 3.1.
- [7] L. Viehland, E. Mason, Transport properties of gaseous ions over a wide energy range, part iv, Atomic Data and Nuclear Data Tables 60 (37-95) (1995) p. 71.
- [8] Y. Kaneko, T. Koizumi, N. Kobayashi, J. Phys. Soc. Japan 43 (1817).
- [9] W. Blum, W. Riegler, L. Rolandi, Particle Detection With Drift Chambers, Springer-Verlag, 2008.
- [10] R. Veenhof, Calculations for the alice tpc read-out.
URL http://rjd.home.cern.ch/rjd/Alice/neon_mobility.html